A Safety Evaluation of Moored Ship Motions by Observed Tsunami Profile

*Ik-Soon Cho[1], Masayoshi Kubo[2], Gil-Young Kong[3] , Yun-Sok Lee[4] and Choong-Ro Lee[5]

[1] Research Institute of Maritime Industry, Korea Maritime Univ.(E-mail: ischo@bada.hhu.ac.kr)
[2] Faculty of Maritime Sciences, Kobe Univ.(E-mail: kubomasa@maritime.kobe-u.ac.jp)
[3] Division of Navigation System Engineering, Korea Maritime Univ.(E-mail: kong@hhu.ac.kr)
[4] The Center of Ship Operation, Korea Maritime Uni. (E-mail: lys@bada.hhu.ac.kr)
[5] Korea Institute of Maritime and Fisheries Technology (E-mail: crlee@seaman.or.kr)

Abstract

Recent warnings indicate that there is a potential risk of massive earthquake in Japan within 30 years. These earthquakes could produce large-scale tsunamis. Tsunamis are very powerful and can be traveled thousands of miles and caused damage in many countries. Consideration of the effect of tsunami to the moored ship is very important because it brings the loss of life and vast property damage. In this paper, the numerical simulation procedure to analyze the motions of a moored ship due to the observed waves of tsunami, Tokachi-off earthquake tsunami profile in northern Pacific coasts of Japan on September 26 in 2003. And the effects on the motions and mooring loads are investigated by numerical simulation. Numerical simulations consist of hydrodynamic analyses in a frequency domain and ship motion analyses in a time domain as the motions of moored ships are examined. As the process begins, the hydrodynamic and wave-exciting forces for moored ships must be calculated. Ship motions and mooring forces can then be calculated by solving the equations of motion. In order to investigate the safety evaluation on the motions of moored ship by tsunami attack, we applied a numerical simulation procedure to a 135,000m^3 LNG carrier moored at an offshore sea berth.

Keywords: Safety evaluation, Moored ship motions, Observed Tsunami, Simulation method

1. Introduction

Tsunamis are a threat to ships entering and departing harbors and mooring; they result in broken mooring lines and ships set adrift. And extremely serious accidents, such as stranded ships and collisions with quays, may also occur. Despite these potentially serious problems, there are currently no studies that deal specifically with numerical simulations of tsunamis and their effects on moored ships.

On the other hand, since the tsunami consists of approximately component waves of several minutes, there is a possibility of resonance with the long-period motion of mooring vessel. As the speed of tsunami is much faster than tidal current in a harbor, a strong resisting force might act on the moored ships.

Mooring problems related to the external forces of observed waves of tsunamis are examined in this paper. Consequently, numerical simulations are proposed to study the motions of moored ships subjected to tsunamis, and the effects of the initial wave are investigated by numerical simulation method, applying to LNG carrier.

2. Observed Data of the Tokachi-off Earthquake Tsunami

The 2003 Tokachi-off earthquake tsunami was appeared on September 26 in 2003. It was reported that the magnitude of the earthquake was 8.0 and the hypocenter was at off-Tokachi of the Hokkaido Pacific side coast with 42km deep under the seabed. The tsunami attacked northern Pacific coast of Japan, including Hokkaido and Tohoku area. Port and Airport Research Institute observed tsunami profile at Tokachi-off(23m deep) and coastal tide station inside the harbor. (Nagai et al, 2004)

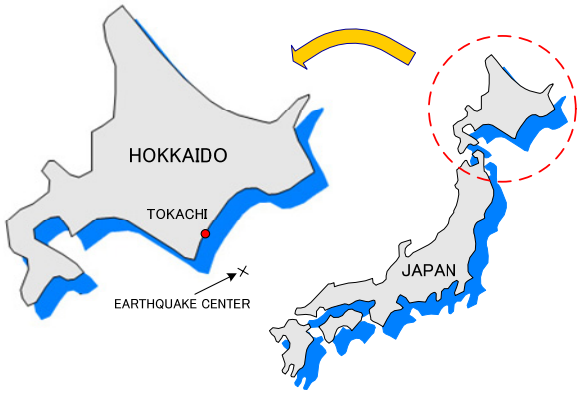

Figure 1. Position of Tokachi area

The observed tsunami profile and currents(three upper figures) and tide level inside Tokachi harbor(lower figure) as shown in Figure 2.

3. Numerical Simulations Applied to Ship Motions

3.1 Outline of the Numerical Simulation Method

Numerical simulations consist of hydrodynamic analyses in a frequency domain and ship motion analyses in a time domain as the motions of moored ships are examined. As the process begins, the hydrodynamic and wave-exciting forces for moored ships must be calculated. Ship motions and mooring forces can then be calculated by solving the equations of motion. There are two types of equations of motion. One is the frequency analysis method considering linear mooring forces and regular external forces, and the other is the time domain analysis method using

numerical integration in each time step. The latter is used to consider non-linear mooring forces and irregular external forces.

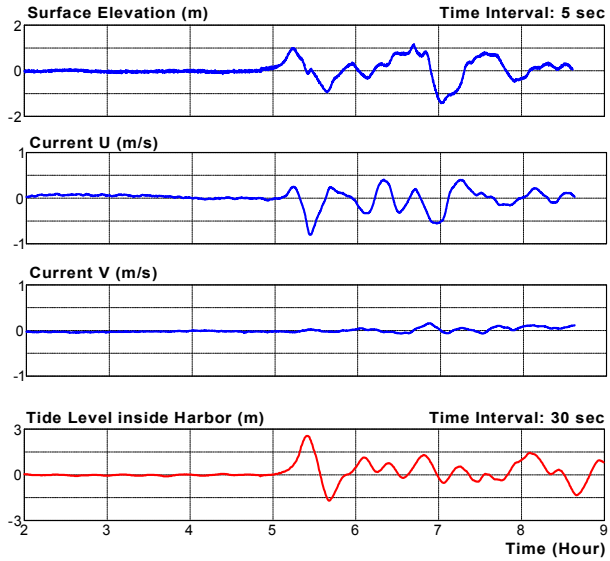

Figure 2. Offshore tsunami profile and tide level inside harbor

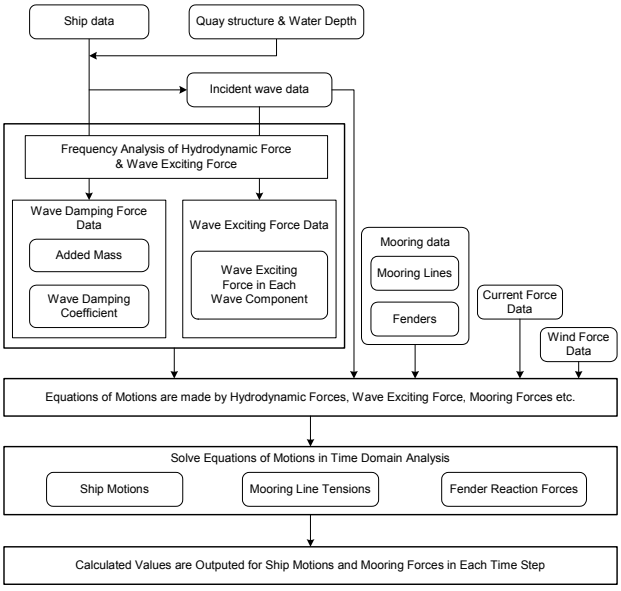

Figure 3. Outline and flow of the numerical simulations

Thus, the time domain analysis is typically used to calculate the motions of moored ships with the use of hydrodynamic and wave-exciting forces that have been calculated by hydrodynamic analysis. Figure 3 shows the outline and flow of numerical simulations in this study. (Kubo et al, 1999)

3.2 Time Domain Analysis of the Motions of Moored Ship

The equation of motions is as follows (Cummins, 1962):

$$\sum_{i=1}^{6}\left\{M_{ij}+m_{ij}(\infty)\right\}\ddot{x}_i(t)+\sum_{i=1}^{6}\left\{\int_{-\infty}^{t}\dot{x}_i(\tau)L_{ij}(t-\tau)d\tau+D_{ij}(t)\right\} \quad (1)$$

$$+\sum_{i=1}^{6}(C_{ij}+G_{ij})x_i(t)=F_j(t) \quad (j=1,2,\cdots,6)$$

where M: ship's mass, $m(\infty)$: constant added mass, $L(t)$: retardation function, $D(t)$: damping force due to mooring lines and viscosity at time t, C: restoring force coefficient, G: mooring force coefficient and $F(t)$: external forces at time t. The suffixed i and j show the mode of ship motions (1~6). The retardation function and the constant added mass are calculated as follows:

$$L_{ij}(t)=\frac{2}{\pi}\int_0^{\infty}B_{ij}(\sigma)\cos\sigma t\,d\sigma \quad (2)$$

$$m_{ij}(\infty)=A_{ij}(\sigma)+\frac{1}{\sigma}\int_0^{\infty}L_{ij}(t)\sin\sigma t\,dt \quad (3)$$

where $A(\sigma)$: added mass at σ, and $B(\sigma)$: damping coefficient at σ.

4. Influence of the Initial Wave of Tsunami on the Moored Ship Motions

4.1 Determination of the Surface Elevation and Current of a Tsunami

At first, a tsunami wave profile is determined, one that contains a surface elevation and currents within a harbor around a target berth. The surface elevation and currents are determined as a time series of observed tsunami profile at Tokachi-off. However, a surface elevation inside a harbor is necessary to evaluate mooring safety. Therefore, the absolute values are modified to coincide with tide level inside harbor. Figure 4 shows the surface elevation at the gravity center of a ship moored at a target berth during 2,500sec. From this figure, the tsunami height is nearly 2.5m. In addition, Figure 5 shows the result of the power spectrum of the surface elevation used in the simulation.

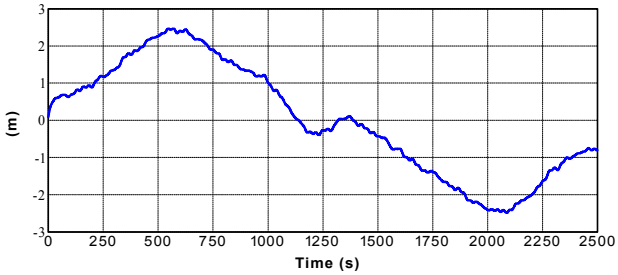

Figure 4. Time series of the surface elevation

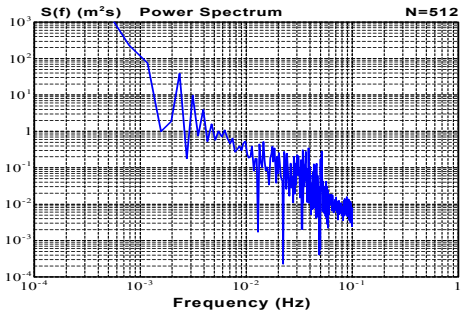

Figure 5. Spectrum result of the surface elevation

4.2 Calculation of the Velocity Potential

Generally, numerical simulations of a tsunami can be used to derive a tsunami profile, which includes the surface elevation and currents at arbitrary positions from the long-wave theory. (Imamura, 1996) On the other hand, the velocity potential at gravity center position can be used to calculate the exciting forces and drag forces as well as the surface elevation. Tsunamis are considered to be a superposition of long waves because the

periods of those component waves are sufficiently long. A calculation procedure in respect to the velocity potential and current velocity calculated by using the surface elevation of tsunami is proposed.

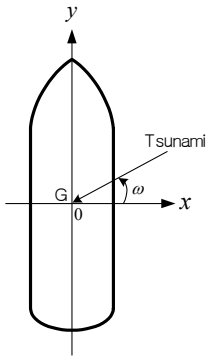

Figure 6. Coordinate system

The coordinate system around the gravity center of ship is set as shown in Figure 6. A tsunami approaches a ship with direction ω to propagate in that direction. The surface elevation and velocity potential of a wave are defined below. (Cho, 2005)

$$\eta(x,y,t)=\frac{1}{g}\frac{\partial\Phi}{\partial t}=i\zeta_0\exp\{ik(x\cos\omega+y\sin\omega)+i\sigma t\} \tag{4}$$

$$\begin{aligned}\Phi=&\sum_{j=1}^{N/2-1}\left[\frac{A_j\sigma_j}{k_j}\frac{\cosh k_j(h+z)}{\sinh k_j h}\sin\left(\sigma_j t+k_j x\cos\omega+k_j y\sin\omega\right)\right]\\&+\sum_{j=1}^{N/2-1}\left[-\frac{B_j\sigma_j}{k_j}\frac{\cosh k_j(h+z)}{\sinh k_j h}\cos\left(\sigma_j t+k_j x\cos\omega+k_j y\sin\omega\right)\right]\\&+\frac{A_{N/2}\sigma_{N/2}}{2k_{N/2}}\frac{\cosh k_{N/2}(h+z)}{\sinh k_{N/2}h}\sin\left(\sigma_{N/2}t+k_{N/2}x\cos\omega+k_{N/2}y\sin\omega\right)\end{aligned} \tag{5}$$

where σ_j is the angular frequency of the j-th component wave, k_j is the wave number, A_j and B_j show the Fourier coefficient of waves.

The water particle velocities for the x and y directions are calculated by differentiating the velocity potential with respect to x and y as in Eqs.(6)~(7).

$$\begin{aligned}u=\frac{\partial\Phi}{\partial x}=&\sum_{j=1}^{N/2-1}\left[A_j\sigma_j\frac{1}{\sinh k_j h}\cos\left(\sigma_j t+k_j x\cos\omega+k_j y\sin\omega\right)\right]\cos\omega\\&+\sum_{j=1}^{N/2-1}\left[B_j\sigma_j\frac{1}{\sinh k_j h}\sin\left(\sigma_j t+k_j x\cos\omega+k_j y\sin\omega\right)\right]\cos\omega\\&+\frac{A_{N/2}\sigma_{N/2}}{2k_j}\frac{1}{\sinh k_{N/2}h}\cos\left(\sigma_{N/2}t+k_{N/2}x\cos\omega+k_{N/2}y\sin\omega\right)\cos\omega\end{aligned} \tag{6}$$

$$\begin{aligned}v=\frac{\partial\Phi}{\partial y}=&\sum_{j=1}^{N/2-1}\left[A_j\sigma_j\frac{1}{\sinh k_j h}\cos\left(\sigma_j t+k_j x\cos\omega+k_j y\sin\omega\right)\right]\sin\omega\\&+\sum_{j=1}^{N/2-1}\left[B_j\sigma_j\frac{1}{\sinh k_j h}\sin\left(\sigma_j t+k_j x\cos\omega+k_j y\sin\omega\right)\right]\sin\omega\\&+\frac{A_{N/2}\sigma_{N/2}}{2k_j}\frac{1}{\sinh k_{N/2}h}\cos\left(\sigma_{N/2}t+k_{N/2}x\cos\omega+k_{N/2}y\sin\omega\right)\sin\omega\end{aligned} \tag{7}$$

The surface elevation of the tsunami, which is given as an irregular wave, is divided into component waves by Fast Fourier Transform(FFT). The currents derived from the tsunami calculation are also divided into components by FFT. From the description of the procedure given above, the surface elevation and currents derived from a tsunami simulation are related to the velocity potential for calculating all of the exciting and drag forces on a moored ship.

4.3 Calculation of the Drag Forces for Ship

The drag forces are determined by using the time series of current as in Eq. (8). (The Overseas Coastal Area Development Institute of Japan, 2002)

$$F_c=0.5\rho_0 C V^2 B \tag{8}$$

where F_c is the drag force, ρ_0 is the density of seawater, C is current pressure coefficient, V is the current velocity and B is the side projected area of the hull below the waterline.

5. Application of the Numerical Model

5.1 Conditions of moored ship

The numerical simulation is applied to an actual vessel in order to investigate the effects of the initial wave of a tsunami on the motions of a moored ship. The moored ship is a 135,000m^3 LNG carrier in an offshore sea berth. The target ship is moored with 16 lines, which are a 42mm-diameter wire rope with a nylon tail rope and 4 pieces fenders(Air Block Fender with Protector Panel) at breasting dolphin as shown in Figure 7. Each line is tested with a tension of 10 tons, and the natural periods of sway and surge are 61 and 146 seconds, respectively, at the initial condition.

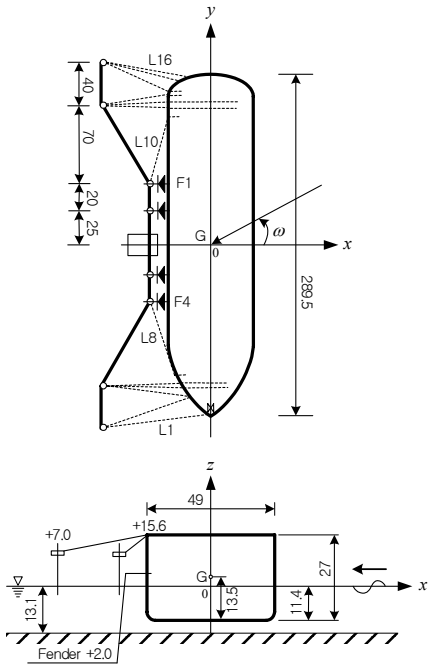

Figure 7. Mooring arrangement of the target ship

Table 1. Details of mooring lines

Name	Diameter	Breaking Tension
Wire ropes	42mm	127ton· f

Table 2. Details of fenders

Name	Type	Max.Deflection
ABF-P 2800H×2800L	Pneumatic	65% (416ton)

5.2 Reproduction by FFT and Abstraction Method of

Components

The surface elevation shows a time series at the gravity center of the ship.

First, the surface elevation is divided into several tsunami wave components by FFT. The number of component wave are determined by the number of data and time interval of the surface elevation,

When reproduction carry out using all component waves, the surface elevation may be not good according to decomposition capability in frequency. That is to say, the short period, which does not exist in a real wave profile, is emphasized, and a reproduction of the long period wave may not be seen. The threshold wave height is then established to select suitable component waves, which are used in the calculation of the exciting and drag forces on a ship. The number of component waves by the setup of a threshold wave height is referred to as *Ne*.

In this paper, the threshold wave height is set at 1.5cm. A number of selected component waves are given as *Ne*=30. When the threshold wave height is 1.5cm, the range of waves in periods is T=2,560s~26s. (Sakakibara et al, 2001)

In this paper, the principal wave direction is set to be only one in order to learn how the initial wave of a tsunami affects a moored ship. Figure 8 shows the principle wave direction derived from the plotting result of the current data of a tsunami. From this figure, it is determined as ω=−6deg.

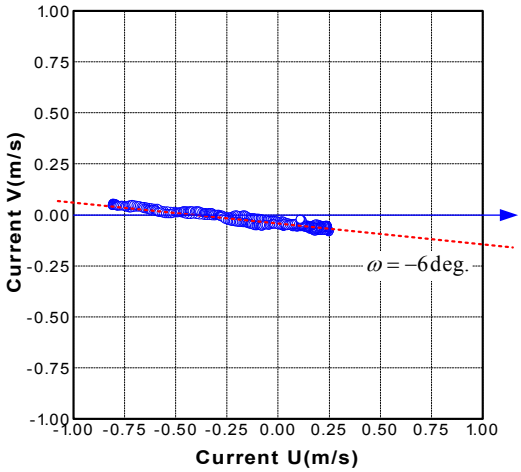

Figure 8. Determination of the wave directions by current data

5.3 Motions of Mooed Ship Using Numerical Simulation Method

A numerical simulation was conducted for a case, threshold wave height=1.5cm and *Ne*=30. Figure 9 shows the calculations of the motions of a moored ship motions. The figure shows that the heave motion is similar to the surface elevation. However, the amplitude of pitch and roll show small value. The spectrum analysis result in the motion of each ship is shown in Figure 10. The value for the peak in each mode is shown in this figure.

Figure 11 shows the calculated mooring line tensions at Line 1(bow line), Line 8(bow spring line), Line 10(stern spring line), Line 16(stern line) and fender 1(stern side), fender 4(bow side). The breaking load of the mooring lines is 127tons. The calculated line tensions exceed the safe working load(42.3tons), which is derived from a safety factor. In addition to line tensions, large reaction forces are generated in all fenders, however, those are within allowable reaction force.

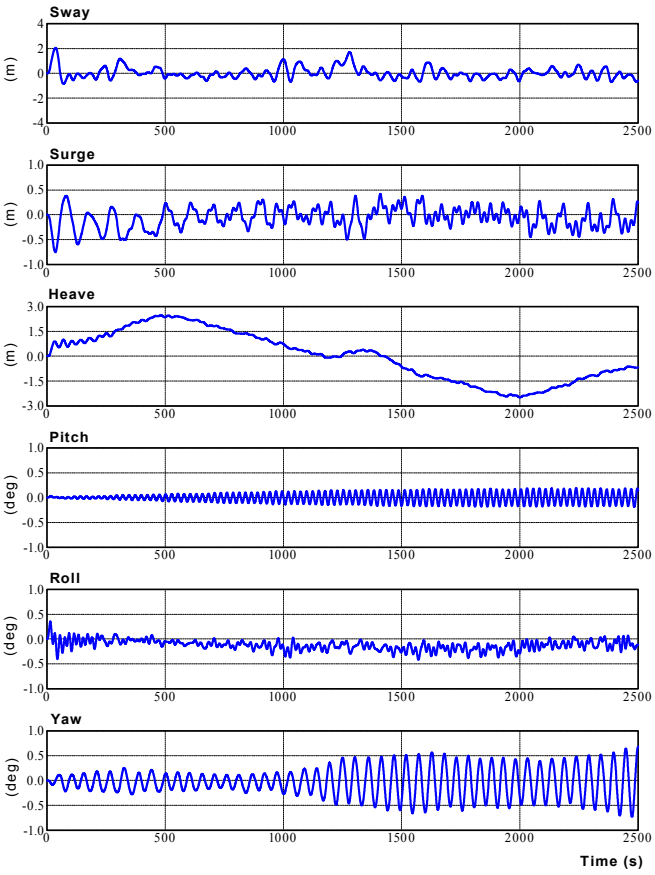

Figure 9. Moored ship motions result

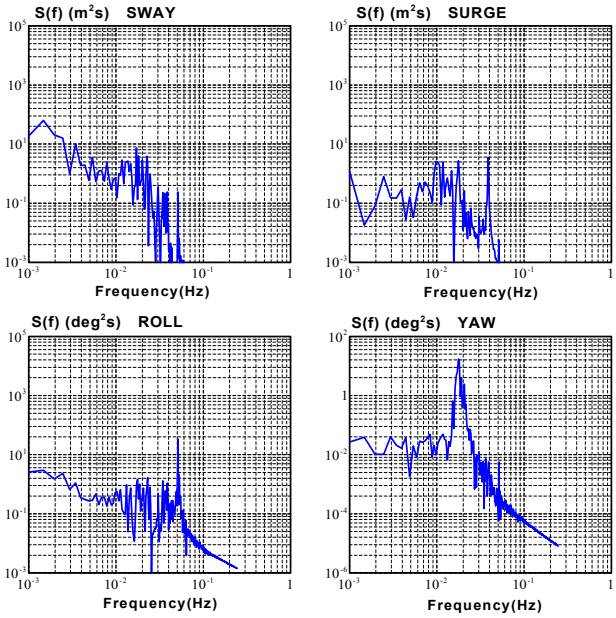

Figure 10. Spectrum results in each ship mode

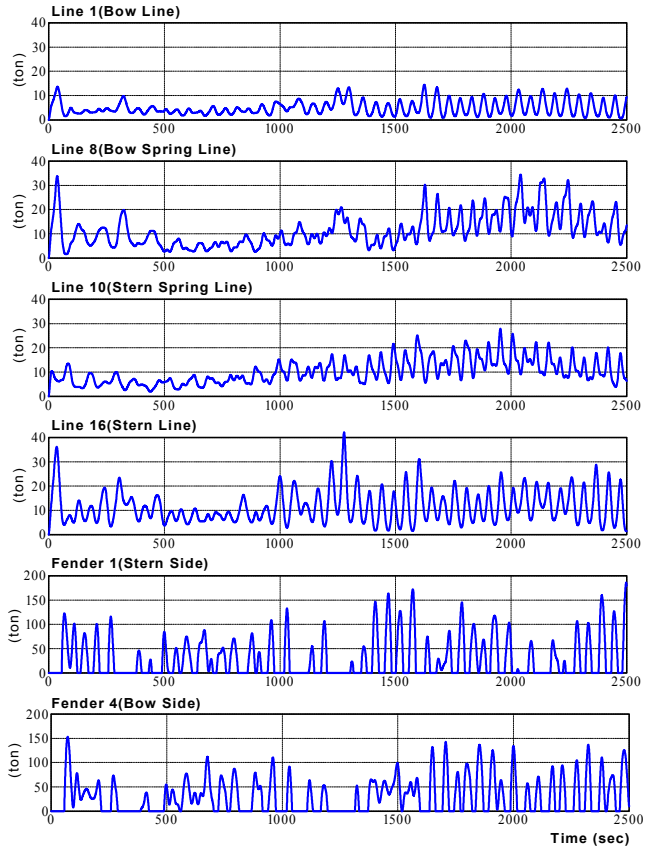

Figure 11. Determination of the wave directions

Table 3 is a summary of the maximum and minimum values for each ship motions. It is found that the movement of the heave attains the height of about five meters. The values of the maximum load on mooring ropes and fenders appear in Table 4.

Table 3. Maximum and Minimum values of ship motions

Ship motions		Values(m)
Sway	Max.	2.051
	Min.	-0.843
Surge	Max.	0.417
	Min.	-0.749
Heave	Max.	2.468
	Min.	-2.486
Pitch	Max.	0.192
	Min.	-0.184
Roll	Max.	0.356
	Min.	-0.416
Yaw	Max.	0.678
	Min.	-0.727

Table 4. Maximum values of mooring loads

Ship motions	Values(ton·f)
Line 1(bow line)	28.94
Line 8(bow spring line)	34.45
Line 10(stern spring line)	27.84
Line 16(stern line)	42.02
Fender 1(stern side)	186.0
Fender 4(bow side)	153.13

6. Evaluation concerning allowable ship motions

Allowable ship motions for cargo handling are defined upper limit of vessel motions at cargo handling at the pier which are given by kinds of vessels and cargo handling method. Ueda and Shiraishi proposed the allowable ship motions based on the investigation of cargo handling troubles. Table 5 shows the allowable ship motions of proposed value presented by Ueda and Shiraishi.(CDIT, 2004) However, Ueda and Shiraishi did not show the allowable ship motions for LNG carrier. Accordingly we applied values of the oversea crude tanker which a target of similar type vessel.

The evaluation method is established as follows.(Sakakibara et al., 1992) First, establish the allowable vessel motions using Tanker-O in Table 5. Second, calculate the ration of interruption, the calculation method of the interruption ratio is assumed as shown in Eq. (8) and Figure 12.

$$Interruption\ ratio(\%) = \frac{excess\ data}{whole\ data} \times 100 \qquad (9)$$

Table 5. Proposal of allowable ship motions for cargo handling

	Surge (m)	Sway (m)	Heave (m)	Roll (deg)	Pitch (deg)	Yaw (deg)
General	±1.0	+1.0	±0.5	±2.5	±1.0	±1.5
Ore carrier	±1.0	+1.0	±0.5	±3.0	±1.0	±1.0
Tanker-D	±1.0	+0.75	±0.5	±4.0	±2.0	±2.0
Tanker-O	±1.5	+0.75	±0.5	±3.0	±1.5	±1.5
Container	±1.0	+1.0	±0.6	±3.0	±1.0	±1.0

Note: General; General cargo vessel, Tanker-D; Domestic tanker, Tanker-O; Oversea crude tanker

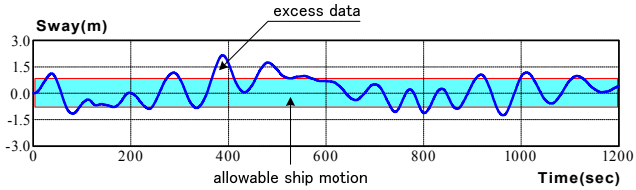

Figure 12. Evaluation for interruption ratio of cargo handling

The above interruption ratio for the numerical simulations in each ship motions are given as Table 6. The ratios for Surge and Heave mode are exceeded more than zero, namely the interruption of the cargo handling will be occurred in this case.

Table 6. Interruption ration in each ship motions

	Sway	Surge	Heave	Pitch	Roll	Yaw
Ratio(%)	8.5	0.0	80.4	0.0	0.0	0.0

7. Conclusion

In this study, the procedure used for the numerical simulation on the motions of a moored ship due to the initial attack of tsunamis and the effect on the motions and mooring loads are investigated. Based on the analysis conducted for this paper, the results are summarized below.

(1) In an observed tsunami, the surface elevation produces large sway and heave motions.

(2) When the highest or lowest water level of a tsunami arrives at the position of the moored ship, the heave

motion attains the maximum upside or downside position, and then sway and surge motions are generated.

(3) When large sway and heave motions are induced at the highest or lowest water level of a tsunami.

(4) The operation efficiency of cargo handling was estimated by the method of interruption ratio. The ratios of Surge and Heave motion are exceeded zero, there is a cargo handling trouble, breakages of mooring ropes and fender damage.

In order to investigate the effects of the initial wave of a large-scale tsunami on the motions of a moored ship, we applied a numerical simulation procedure to a 135,000 m^3 LNG carrier moored at an offshore sea berth.

More detailed examinations will be necessary to clarify the effects of tsunamis on the shipping industry. Details, such as the type of ship, size, mooring system, condition of ship, and ballast, should be examined so that countermeasures against such powerful forces of nature can be implemented.

Reference

1. I.S. Cho, “A Study on the Evaluation of Ship Operatio ns Safety within a Harbor under the Effects of Waves and Tsunami,” *Doctoral Thesis, Kobe University*, 2005, pp. 93~118.
2. W.E. Cummins, “Impulse Response Function and Ship Motions,” *Schiffstechnik, Bd.9, Heft 47*, 1962, pp. 101~10 9.
3. M. Kubo and S. Sakakibara, “A Time Domain Analysis of Moored Ship Motions Considering Harbor Oscillations,” *Pr oceeding of the 9th International Offshore and Polar Engineering Conference,* Vol. 3, No. 5, 1999, pp. 574~581.
4. S. Sakakibara, K. Saito and M. Kubo, “A Study on Long-Period Moored Ship Motions in a Harbor Induced by a Resonant Large Roll Motion under Long-Period Wav es,” *Proceeding of the 11th International Offshore and Polar Engineering Conference,* Vol. 3, 2001, pp. 326~333.
5. S. Sakakibara, and M. Kubo, “Influence of Fender type on Operation Efficiency of Cargo Handling,” *10th IHC,* 1992, pp. 4.19~4.23.
6. Coastal Development Institute of Technology(CDIT), “Manual to evaluate the effect of long-period waves in the ports”, *Coastal Development Technology Library,* No.21, 2004, p. Appendix A-1.(in Japanese)
7. The Overseas Coastal Area Development Institute of Ja pan, “Technical Standards and Commentaries for Port a nd Harbour Facilities in Japan,” 2002, pp. 23~27.
8. T. Nagai, H.Ogawa, “Characteristic of the 2003 Tokachi-off Earthquake Tsunami Profile”, *Technical Note of the Port and Airport Research Institute*, 2004, pp. 1~43.